Crystal Structure of MCM-65: An Alternative Linkage of Ferrierite Layers

Douglas L. Dorset* and Gordon J. Kennedy

Corporate Strategic Research, ExxonMobil Research and Engineering Company, 1545 Route 22 East, Annandale, New Jersey 08801

Received: April 22, 2004; In Final Form: June 15, 2004

The crystal structure of calcined MCM-65 was determined by constrained model building suggested by a close comparison with as-synthesized MCM-47. Synthesized with a compact structure-directing agent (quinuclidine), as-synthesized MCM-65, unlike MCM-47, is found to retain its crystallinity after calcination. It crystallizes in space group *Cmcm*, where $a = 7.373$ Å, $b = 18.006$ Å, and $c = 13.849$ Å and represents a linkage of ferrierite layers oriented in a common direction to form a two-dimensional microporous structure of orthogonal eight-membered ring channels with respective dimensions 4.4×2.6 Å and 4.6×2.7 Å. Rietveld refinement of the model against synchrotron powder diffraction data ($\lambda = 1.15201$ Å) gives $R_{wp} = 0.12$, $R(F^2) = 0.21$. The crystal density is 1.95 g/cm^3, and the framework density for T sites is 19.4. Solid-state ^{29}Si NMR data for the as-synthesized MCM-65 are in agreement with the proposed structure and indicate that the silanol groups are linked after calcination. Although the structure-directing agent has a significant influence on calcination behavior it is found, e.g., by electron diffraction experiments, that MCM-47, MCM-65, ZSM-52, and ZSM-55 form a family of closely similar materials.

Introduction

It is generally recognized that zeolites comprise a class of microporous materials that are quite useful for industrial catalysis and separations.[1] In the search for new porous geometries, layered materials have been considered, a notable example[2] being MCM-22. This material has been shown to link two-dimensional sheets into a three-dimensional cage structure upon calcination. Its crystal structure has been determined,[2] also in its all-silica form,[3] and compared with that of MCM-49, which appears to be somewhat similar,[4,5] although directly synthesized as the three-dimensional cage.

Another class of layered materials considered recently is that related to the zeolite ferrierite[6] (FER). By control of synthetic conditions, it is possible to make a precursor, viz., the so-called pre-ferrierite[7] (PREFER). Upon calcination of the precursor, the adjacent two-dimensional sheets, related by mirror symmetry, link into the FER cage structure. In the context of characterizing precursors to layered silicates, the crystal structure of as-synthesized MCM-47[8] was recently determined.[9] Individual ferrierite layers in this crystalline material have a common orientation rather than a mirror relationship between nearest layers. Attempts to calcine this material markedly degraded the sample crystallinity, and attempts were made to explain this loss of order with models in which only half of the silanol groups were involved in cross-layer links. Another material containing ferrierite layers, MCM-65, can be readily calcined into another crystalline material.[10] Its powder X-ray diffraction pattern is found to share many spacings in common with that of MCM-47, although the intensity distribution is different.

The crystal structure of calcined MCM-65 is described in this report, first showing that the as-synthesized material is quite similar to that of MCM-47. However, the calcined material represents a new cage structure comprising a two-dimensional network of eight-membered ring channels.

* Correponding author. E-mail: d.l.dorset@exxonmobil.com.

Materials and Methods

Zeolites. MCM-65 was synthesized as described in a recent patent.[10] This aluminosilicate was prepared via quinuclidine and tetramethylammonium hydroxide as structure-directing agents (SDAs). In this study, as-synthesized and calcined forms were characterized. By contrast, the aluminosilicate, MCM-47, was originally synthesized using tetramethylene bis-(*N*-methyl pyrrolidinium) dibromide as the SDA following the procedure of Valyosik.[8] The zeolites ZSM-52[11] and ZSM-55,[12] respectively an aluminosilicate and a borosilicate, were synthesized using choline chloride as the SDA. A commercial sample of ferrierite was used for electron diffraction studies. (In this study of related materials, i.e., MCM-65, ZSM-52, and ZSM-55, SDA-containing material is designated "as-synthesized", whereas "calcined" material contains no SDA. MCM-47, on the other hand, is understood to contain SDA.)

Powder X-ray Diffraction. Debye−Scherrer X-ray diffraction measurements on MCM-65 as-synthesized and calcined powder samples in capillaries ($\lambda = 1.15201$ Å) were made at the ExxonMobil beamline X10B at the Brookhaven National Laboratory. Bragg−Brentano powder diffraction measurements on as-synthesized and calcined ZSM-52 and ZSM-55 (Cu Kα radiation) were carried out by Dr. J. Vartuli on a Scintag diffractometer. Patterns were indexed with the Jade software package from MDI, Inc. Rietveld refinements of structural models were made with GSAS.[13] Silicate models used for Rietveld refinement were first refined by DLS[14] to optimize bonding parameters.

Electron Diffraction. Transmission electron diffraction measurements were carried out at 200 kV with a JEOL JEM-2010 electron microscope. Zeolite samples were first crushed to fine powders in a mortar and pestle and then suspended in acetone in an ultrasonic bath. Drops of the fine particle suspension were then dried on carbon-film-covered 300-mesh copper electron microscope grids. Diffraction patterns were recorded on Kodak SO-163 electron microscope film developed

10.1021/jp040305q CCC: $27.50
Published on Web 08/21/2004

in Kodak HRP developer. Diffraction patterns were calibrated against a gold powder standard for measurement of reciprocal spacings. Intensity data were extracted from patterns digitized on a flat-bed scanner via the ELD[15] software.

In some cases, direct methods were used to test zonal electron diffraction data from various zeolites to ascertain that they would correspond to the known structures. For this purpose, Σ_1- and Σ_2-three-phase structure invariants were evaluated, as described by Hauptman.[16] Comparisons of a structural model to the electron diffraction intensities sometimes required the use of a secondary scattering correction[17] to demonstrate convergence.

NMR Spectroscopy. All of the solid-state NMR measurements were done at room temperature. The ^{29}Si MAS and CPMAS NMR data were recorded on a Varian Infinity Plus 500 wide-bore spectrometer operating at a static magnetic field of 11.7 T, corresponding to a Larmor frequency of 99.3 MHz. The ^{29}Si spectra were recorded on samples of the as-synthesized and calcined MCM-65 that were loaded in 7.5-mm (o.d.) MAS PENCIL rotors, spinning at the magic angle at rates of about 4 kHz with ^{1}H decoupling during data acquisition, 4-μs pulses, and a 120-s pulse delay, with 240−640 scans collected. ^{29}Si CP/MAS data were recorded with magic-angle spinning rates of about 3.5 kHz, ^{1}H decoupling during data acquisition, 4.5-μs $\pi/2$ pulses, a 3.5-ms contact time, and a 5-s pulse delay, with 2400−4800 scans collected. The ^{13}C CPMAS NMR spectra were recorded on a Bruker AMX360 wide-bore spectrometer operating at a static magnetic field of 8.4 T, corresponding to a Larmor frequency of 90.56 MHz. Spectra were recorded on samples of the as-synthesized MCM-65 loaded in 7.5-mm (o.d.) MAS PENCIL rotors, spinning at the magic angle at rates of about 3 kHz with ^{1}H decoupling during data acquisition, 6-μs $\pi/2$ pulses, a 1.5-ms contact time, and a 2-s pulse delay, with 4800 scans collected. The ^{1}H MAS NMR spectra were obtained on a Bruker AMX360 (8.6T) NMR spectrometer corresponding to a Larmor frequency of 360.13 MHz. Spectra were recorded with a 4-mm MAS probe using a 10.0−15.0 kHz spinning, 3.0−4.0-μs 90° pulses, a 30-s pulse delay, and averaging of 32 scans. The amount of H in each sample was determined by directly comparing the experimental spectral area to that of an external standard and normalizing by weight.

A full rotor of octakis(trimethylsiloxy)silesquioxane, more commonly known as Q8M8, was used as the external quantitation standard. This material is solid at room temperature, has tuning characteristics similar to those of the materials of interest, and has one peak at about 0.3 ppm from TMS. Q8M8 was obtained from Strem Chemicals (CAS# 51777-38-9). The standard and the samples were run back to back under identical conditions to minimize any effects due to spectrometer instability. Measurements done in quadruplicate on these and experimental samples give a standard deviation of <4% for this methodology. Chemical shifts for ^{1}H, ^{13}C, and ^{29}Si were calibrated using TMS ($\delta_H = 0$ ppm, $\delta_C = 0$ ppm, and $\delta_{Si} = 0$ ppm).

Prior to the ^{1}H NMR measurements, samples are packed in 4-mm (o.d.) ZrO_2 MAS rotors and placed in a horizontal quartz tube that is attached to a vacuum line. Typically, to avoid bumping of the samples, the quartz tube containing packed rotors is slowly evacuated to 10^{-3} Torr at room temperature. The tube is then heated in a tube furnace to 100 °C at 1 °C/min, held at 100 °C for 1 h, ramped to 400 °C at 2 °C/min, held at 400 °C for 10 h, and then cooled to room temperature under vacuum. The tube is sealed off under vacuum and transferred to a glovebox, and the rotors are then capped under N_2. All packed rotors are stored in the glovebox until used to obtain NMR data. Weights are recorded at each step of the sample preparation for weight normalization of the NMR signals.

Results

Synchrotron powder X-ray diffraction patterns from as-synthesized and calcined MCM-65 are shown in Figure 1. Diffraction peaks extend to 1.7 Å for the former and 1.8 Å for the latter. Pattern indexing reveals that the two materials might have the same space group, *Cmcm* or $Cmc2_1$, also indicated earlier[9] for MCM-47. The unit cell constants are $a = 7.367$ Å, $b = 22.516$ Å, $c = 13.869$ Å and $a = 7.372$ Å, $b = 18.006$ Å, $c = 13.894$ Å for as-synthesized and calcined MCM-65, respectively. It should be noted that the parameters for the as-synthesized material match closely those for MCM-47 ($a = 7.393$ Å, $b = 22.461$ Å, $c = 14.030$ Å) and that calcination of the material involves a shortening of just the *b* axis by 4.5 Å, again while preserving the space group symmetry. Two of the cell constants are also in close agreement with the values found for ferrierite[6] in space group *Immm*, even though there is a change in zonal symmetry from primitive to *c*-centered while projecting down the longest unit cell axis.

Electron diffraction measurements on MCM-47, MCM-65, ZSM-52, ZSM-55, and ferrierite (FER) (Figure 2) reveal, first, that the first group of materials is different from FER, i.e., although patterns from all substances correspond to a rectangular projection with dimensions near 13.8 × 7.2 Å, only the zonal patterns from FER have *c*-centered symmetry. A kinematic structure factor calculation based on the known structure[6] of FER accounts for the observed electron diffraction intensities ($R_I = 0.34$, $R_F = 0.40$), especially after a correction for secondary scattering[17] ($R_F = 0.22$). (Here, $R = \sum||F_o| - k|F_c||/\sum|F_o|$, scaled (I,F) such that $\sum I_o = \sum I_c$ or $\sum F_o = \sum F_c$.) Direct phase determination of these zonal data finds one set with 23 derived phase values containing only five discrepancies from the zonal model. The reason for this successful analysis is the strong resemblance between the calculated and observed Patterson functions based on electron diffraction intensities.[18]

In the projections nearly parallel to the longest cell axis, it is virtually impossible to distinguish electron diffraction patterns from MCM-47, MCM-65, ZSM-52 ,and ZSM-55. Because of possible slight tilts of their microcrystals, two patterns are commonly observed. One of these (Figure 2b) corresponds to the calculated [010] zone of MCM-47. Using the crystal structure model,[9] there is a close agreement, e.g., with intensity data from MCM-65 where $R = 0.25$ after a correction for secondary scattering. Similarly, the calculated [−110] zone of MCM-47, which is tilted with respect to the previous zone by 18.2°, matches observed patterns from MCM-65, ZSM-52, and ZSM-55 (Figure 2c), e.g., for ZSM-52, $R = 0.23$ after a correction for secondary scattering. Direct determinations of crystallographic phases[16] for both zonal projections are successful, again resulting in models that closely resemble the corresponding MCM-47 projections.

Next, the possible structural identity of MCM-47 and as-synthesized MCM-65 was tested via a Rietveld refinement[13] against the MCM-65 precursor synchrotron powder diffraction data in space group *Cmcm* (Figure 1a). Even though the organic residue is different for MCM-65, the MCM-47 model with a disordered 1,1-dimethylcyclopentane fragment[9] began to fit the intensity profile of the MCM-65 precursor pattern [$R_{wp} = 0.23$, $R(F^2) = 0.24$]. The refinement was not carried out to completion but was only used to verify structural similarity.

From the body of information given above, only one parameter change should be used to seek the structure of

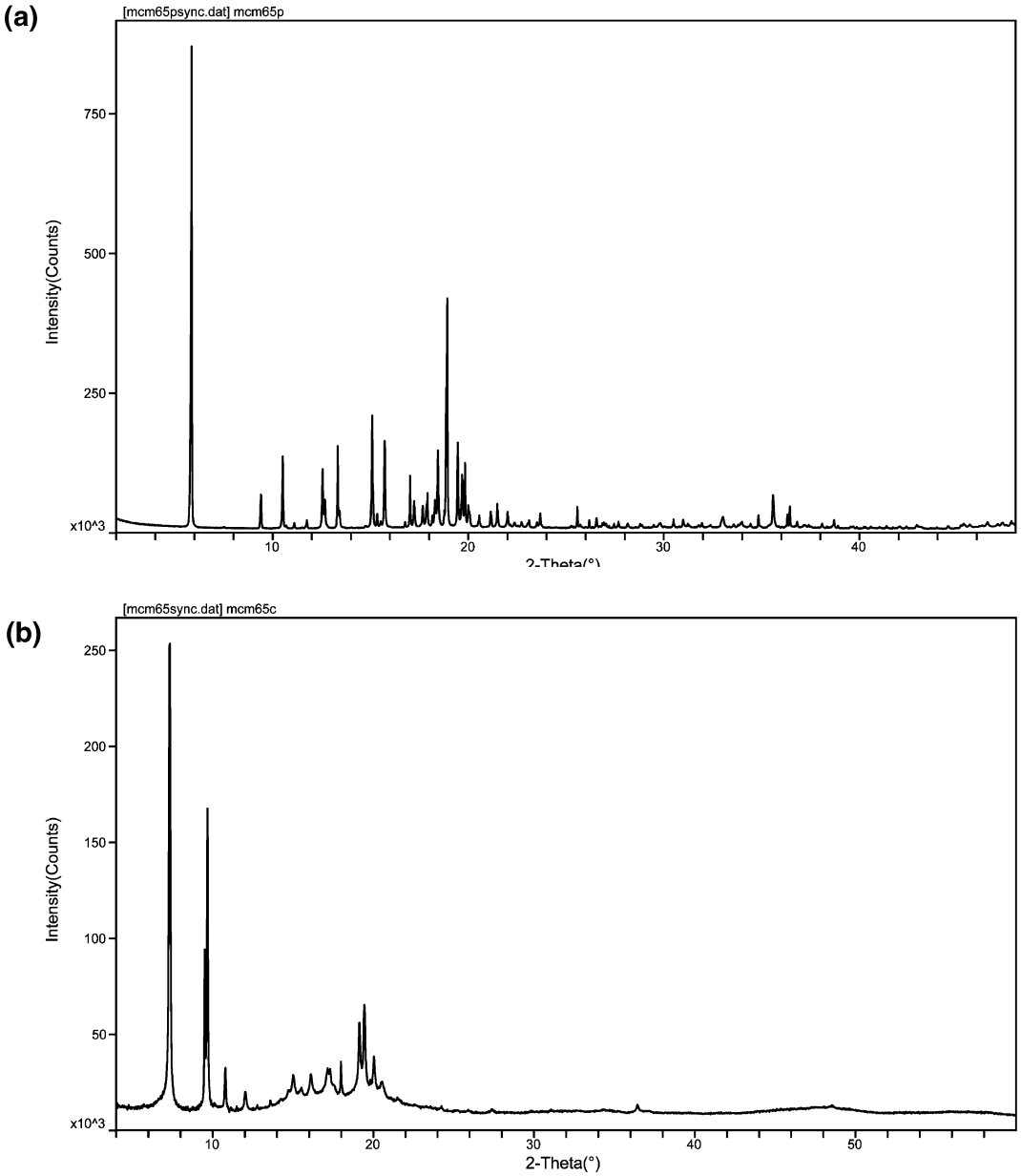

Figure 1. Synchrotron powder data from (a) as-synthesized and (b) calcined MCM-65.

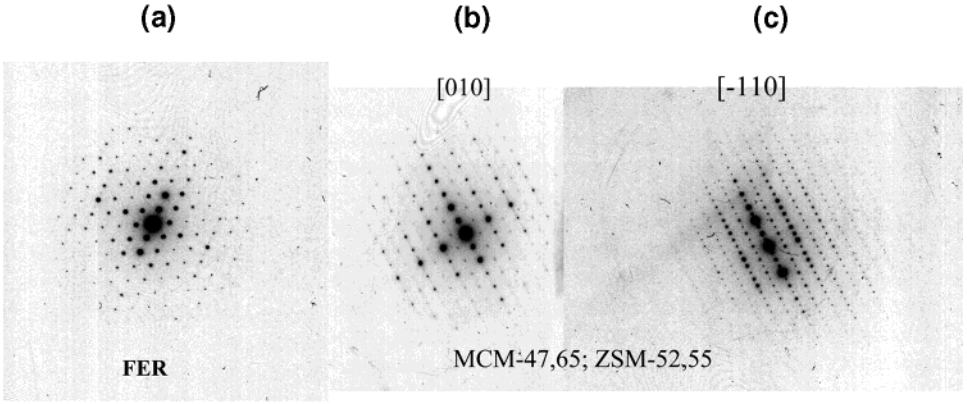

Figure 2. Electron diffraction patterns. (a) Ferrierite, (b,c) ZSM-52, ZSM-55, MCM-47, and MCM-65 all diffract to produce *h*0*l* or *hhl* nets that are virtually indistinguishable from one another.

calcined MCM-65, viz., compression of the *b* axis. With the preservation of the space group symmetry, there is no evidence for symmetry-breaking disorder during calcination of the type proposed by Burton et al.[9] The one-dimensional unit cell compression causes all of the free silanols to form Si−O−Si links across the proximate ferrierite sheets, thus creating asymmetric eight-membered ring channels that are perpendicular to intersecting eight-membered ring channels (Figure 3) in a

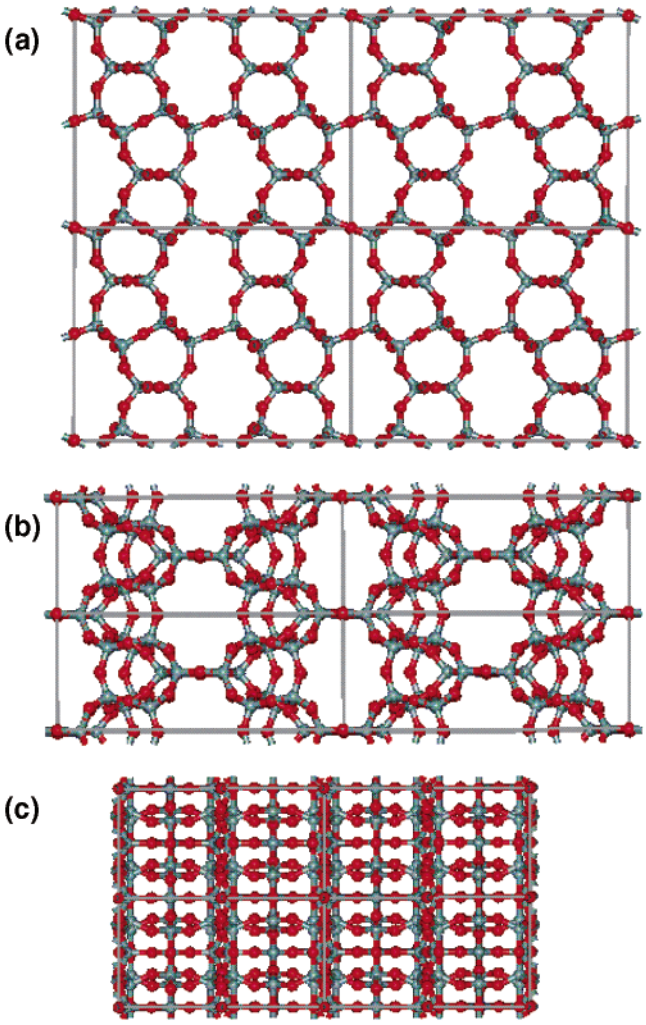

Figure 3. Structural model for calcined MCM-65: (a) [100], (b) [001], (c) [010] projections. The latter projection is the one often encountered in electron diffraction experiments, explaining why calcined and as-synthesized material might produce similar patterns.

two-dimensional porous framework. The appearance of the [010] projection model is reminiscent of the direct methods solution for MCM-47 (Figure 4a in ref 9). DLS refinement[14] of the resulting model results in a residual $R = 0.012$ if unit cell axes are constrained. When axial constraints are removed, $R = 0.0059$, and the cell lengths expand to $a = 7.5602$ Å, $b = 18.7164$ Å, and $c = 14.1037$ Å, corresponding to 2.5%, 3.8%, and 1.8% expansions of the cell along the respective axes.

Rietveld refinement of the calcined MCM-65 model was then carried out in space group *Cmcm* against the synchrotron powder diffraction data. Note that, unlike the earlier refinement of MCM-47, where a low-angle region of the pattern, including a large diffraction maximum, was omitted,[9] a continuous region pattern of calcined MCM-65 from 5° to 40°, containing the complete salient diffraction information, was used. (The figures of merit found in our refinement therefore strive to avoid selected bias.) After fitting of the pattern background, scale factor, zero-point shift, and peak profile parameters, the atomic thermal parameters and positions were then refined. Restraints were imposed on the temperature factors to retain a common value, separately, for Si or O atoms. The refined geometry of the SiO_4 tetrahedron imposed soft bond restraints where Si−O and O−O distances were initially confined within 1.61(3) and 2.65(6) Å, respectively, wherein a restraint factor was gradually relaxed. Agreement between the model and observed data is indicated in Figure 4, corresponding to $R_{wp} = 0.12$, $R(F^2) = 0.21$. No evidence was found for solvent molecules or cations in difference electron density maps. [One observes (Figure 1b) that some peak broadening is introduced by calcination so that the Rietveld refinement suffers somewhat by attempting to model certain fine details that are lost from the experimental powder pattern. Calcined MCM-65 is nevertheless a much more highly ordered, crystalline material than that found in attempts[9] to calcine MCM-47.]

TABLE 1: Fractional Coordinates for Calcined MCM-65 after Rietveld Refinement[a]

atom	*x*/*a*	*y*/*b*	*z*/*c*
Si1	0.21108	0.23554	0.25000
Si2	0.29158	0.17568	0.05342
Si3	0.00000	0.08070	0.53927
Si4	0.00000	0.13565	0.75000
O5	0.19569	0.18057	0.15834
O6	0.00000	0.26616	0.25000
O7	0.32979	0.30844	0.25000
O8	0.19021	0.11060	−0.00107
O9	0.50000	0.14984	0.05586
O10	0.25000	0.25000	0.00000
O11	0.00000	0.08096	0.65751
O12	0.50000	0.50000	0.50000

[a] All Uiso assumed to be 0.025 Å^2.

Final coordinates for the calcined MCM-65 model are reported in Table 1, and bond distances and angles are listed in Table 2. The coordination sequence and vertex symbols are listed in Table 3. The framework density (T sites/1000 Å^3) is 19.4, comparable to those of TON (19.7) and VET (19.8), other frameworks in which a five-membered ring constitutes the smallest unit.[19] The Si−O bond distances lie in the range 1.55−1.65 Å, identical to the result[9] for MCM-47. There is a broader distribution of O−T−O angles than found for MCM-47, viz., 108.8° ± 7.2° vs 109.7° ± 3.7°. T−O−T angles range from 135.2° to 162.4°, where the typical value should be 145°. Values at 180° might represent an average over an infinite set of displaced O positions with varying occupancies.[20]

Motivated by the marked similarity of the electron diffraction patterns from ZSM-52 and ZSM-55 to those from MCM-47 and MCM-65, laboratory powder X-ray data from these materials were indexed with the Jade software. Earlier X-ray studies[21] have shown that ZSM-52 and ZSM-55 should be isostructural. Both materials appear to crystallize in C-centered orthorhombic unit cells with respective dimensions of $a = 7.816$ Å, $b = 21.235$ Å, $c = 14.102$ Å and $a = 7.792$ Å, $b = 21.976$ Å, $c = 13.968$ Å, representing a slight *a*-axis expansion compared to as-synthesized MCM-65 and MCM-47. A pattern from calcined ZSM-52 also was indexed to give $a = 7.4332$ Å, $b = 18.2857$ Å, $c = 13.8034$ Å, closer dimensionally to calcined MCM-65 and also indicating space group *Cmcm* to be a possible unit cell symmetry. The peaks are quite broad in this latter pattern. Nevertheless, the calcined MCM-65 model formed the basis of a trial Rietveld refinement.[13] Although the refinement could not be completed, it is quite probable, from the initial fit [$R_{wp} = 0.15$, $R(F^2) = 0.19$], that the ordered regions of calcined ZSM-52 and calcined MCM-65 are very similar.

The ^{29}Si MAS and CPMAS NMR spectra of as-synthesized MCM-65 are shown in Figure 5a. Four resonances are observed at $\delta = -105.7$, -109.3, -111.0, and -114.1 ppm from TMS. The -109.3 ppm peak represents approximately 7% of the total spectral area, is very sharp compared to the other three resonances, and is consistent with the presence of an impurity such as cristobalite or quartz. (The powder diffraction evidence does not clearly indicate such an impurity, although the presence

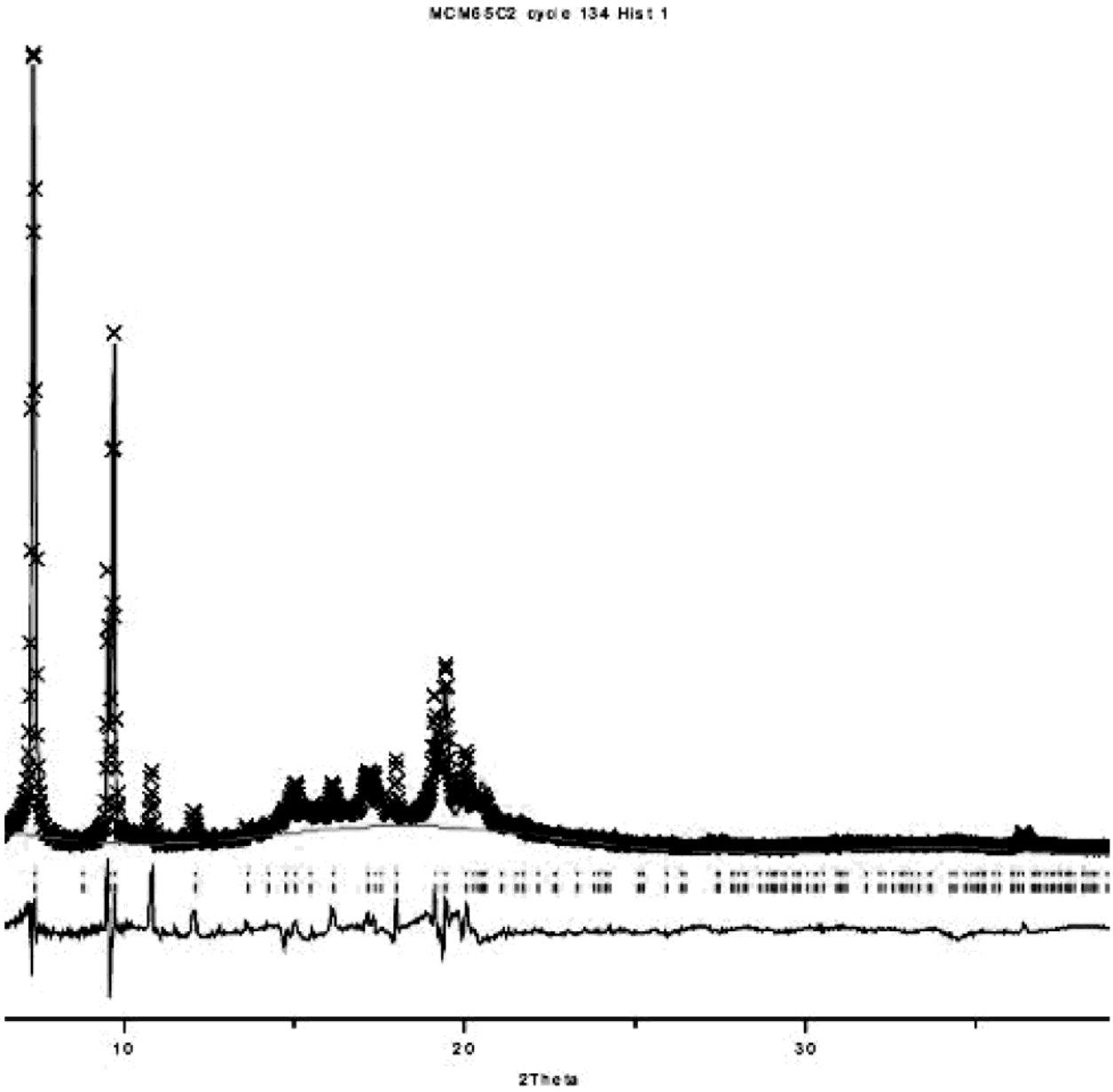

Figure 4. Rietveld refinement results for calcined MCM-65 based on the structure in Figure 3.

of quartz cannot be ruled out.) Assuming that this assignment is correct, the other three peaks can be assigned to the various crystallographically distinct T sites in the proposed structure of the as-synthesized MCM-65 precursor. Deconvolution of the MAS NMR spectrum indicates that ~22% of the Si atoms are associated with the peak at −105.7 ppm, ~39% with the peak at −111.0 ppm, and ~39% with the peak at −114.1 ppm. The chemical shift, observed population (22% predicted from model), and $^{1}H \rightarrow {}^{29}Si$ cross-polarization (CP) enhancement of the −105.7 ppm peak confirm that it is associated with hydroxyls and can be assigned to the $T_3(8)$ site. Likewise, the peak at −111.0 ppm can be assigned to the sum of $T_1(8)$ and $T_4(4)$ sites, and the peak at −114.1 ppm to the $T_2(16)$ site.

The ^{29}Si MAS and CPMAS NMR spectra of calcined MCM-65 are shown in Figure 5b. Comparison of these spectra indicates that there are very few residual hydrogens available for $^{1}H \rightarrow {}^{29}Si$ cross-polarization, unlike the case of calcined MCM-47 where a large proportion of the silanols remain. This observation is consistent with the condensation of the silanols in adjacent layers upon calcination proposed by the above crystal structure analysis. In fact, ^{1}H MAS NMR data show that there is less than 0.3 mmol of OH/g in the calcined MCM-65 material. This is characteristic of a fully condensed microporous zeolite. Comparison of the ^{29}Si MAS spectra of as-synthesized and calcined MCM-65 in Figure 5a,b shows significant spectral broadening upon calcination. This is often indicative of a loss of crystallinity, as in the case of calcined MCM-47, or local disorder. However, the diffraction data indicate that a mostly ordered crystalline framework is maintained in MCM-65 upon calcination. Thus, an alternative explanation of the Si NMR spectral broadening is that there is a much broader distribution of local environments in the calcined material than in the as-synthesized parent. This would be manifested as a continuum of overlapping peaks rather than a series of distinct resonances.

The ^{13}C CPMAS NMR spectrum of as-synthesized MCM-65 is shown in Figure 6. This spectrum demonstrates that the SDAs (quinuclidine and TMA^{+}) are intact and fairly rigidly held in the voids of the MCM-65 precursor.

Discussion

The crystal structure of calcined MCM-65 has been found to comprise a two-dimensional network of eight-membered ring

TABLE 2: Bond Distances (Å) and Angles (°) for MCM-65 Compared to MCM-47

bond	MCM-65	MCM-47
Si1−O5	1.61	1.58
Si1−O6	1.65	1.58
Si1−O7	1.58	1.55
Si2−O5	1.62	1.63
Si2−O8	1.58	1.57
Si2−O9	1.60	1.58
Si2−O10	1.56	1.57
Si3−O8	1.59	1.60
Si3−O11	1.64	1.61
Si3−O12	1.55	1.65
Si4−O7	1.61	1.55
Si4−O11	1.61	1.59
angle	**MCM-65**	**MCM-47**
O5−Si1−O5	103.7	104.8
O5−Si1−O6	97.9	109.0
O5−Si1−O7	123.3	112.1
O6−Si1−O7	104.2	109.6
O5−Si2−O8	105.2	109.7
O5−Si2−O9	114.5	111.3
O5−Si2−O10	107.1	108.1
O8−Si2−O9	104.3	103.9
O8−Si2−O10	108.4	111.3
O9−Si2−O10	116.5	112.5
O8−Si3−O8	123.4	114.8
O8−Si3−O11	109.3	107.8
O8−Si3−O12	101.6	110.2
O11−Si3−O12	110.7	105.5
O7−Si4−O7	102.5	118.9
O7−Si4−O11	112.4	107.4
O11−Si4−O11	104.9	108.2
Si1−O5−Si2	135.2	148.0
Si1−O6−Si1	141.0	156.3
Si1−O7−Si4	162.4	152.1
Si2−O8−Si3	145.6	151.2
Si2−O10−Si2	180.0	180.0
Si3−O11−Si4	142.6	160.1
Si3−O12−Si3	180.0	−

TABLE 3: Coordination Sequence and Vertex Symbols for Calcined MCM-65

atom	coordination sequence[27]	vertex symbol[28]
Si1(8 m)	4 12 20 35 69 105 125 168 231 282	$5\ 5_2\ 5\ 5_2\ 8\ 7_2$
Si2(16 1)	4 12 21 39 67 99 129 172 228 275	5 5 5 5_2 5 8
Si3(8 m)	4 12 28 44 64 100 144 178 215 277	$5\ 8_2\ 5\ 8_2\ 5_2\ 8_2$
Si4(4 2mm)	4 12 24 42 66 98 130 172 228 278	$5\ 5\ 5\ 5\ 5_2\ 8_2$

channels. Taking the van der Waals radii of silicon and oxygen atoms[22] into account, the set of asymmetric channels formed by the linkage free silanols have dimensions 4.4 × 2.6 Å. The orthogonal channel openings measure 4.6 × 2.7 Å. These dimensions are in accord with those of other microporous materials with eight-membered rings[1].

These results, combined with the previous study[9] of MCM-47, indicate that the ease of calcination, and hence the crystallinity of the final product, depends somehow on the nature of the structure-directing agent. For MCM-65, it can be shown that the crystallinity of the calcined product does not decrease drastically upon removal of the organic. (The diffraction limit of *strong* diffraction lines near $d = 3.0$ Å merely is a characteristic of this cage structure, as revealed by model calculations. All maxima beyond this resolution are rather weak, especially when no correction is made to the intensities for a Lorentz factor, so that any reasonable atomic temperature factor would further diminish their visibility. Yet weak peaks are observed out to $d = 1.8$ Å.) In addition, the diffraction lines from the calcined MCM-65 sample are rather sharp.

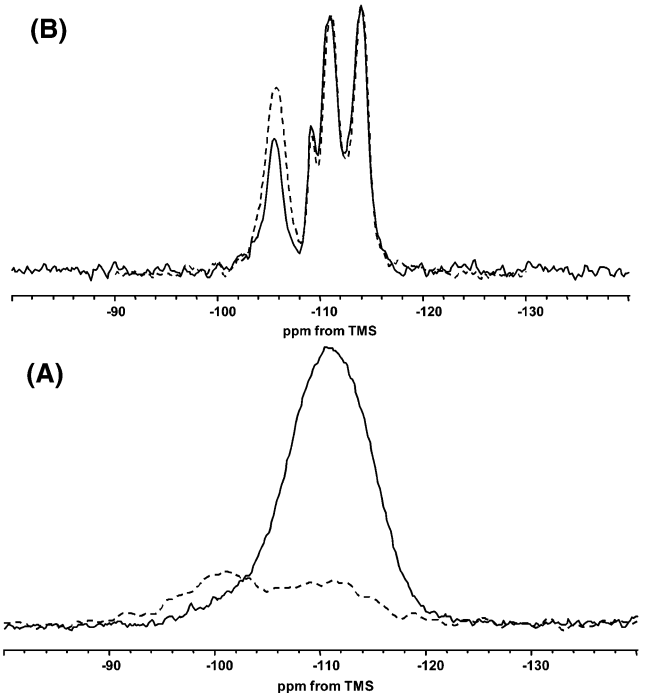

Figure 5. ^{29}Si MAS (—) and ^{29}Si CPMAS (− − −) spectra of (A) as-synthesized and (B) calcined MCM-65.

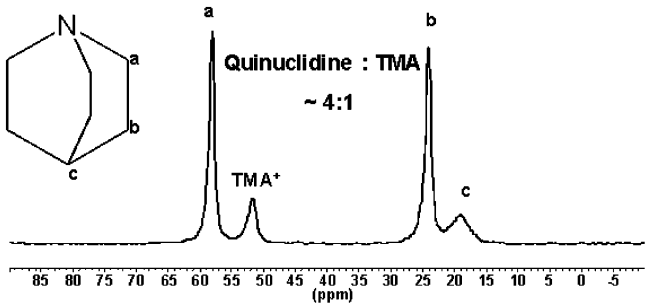

Figure 6. ^{13}C CPMAS NMR spectrum of as-synthesized MCM-65.

In the study of a related structure, the diffraction lines from calcined ZSM-52 are quite broad, with observed diffraction maxima extending to 3.1 Å, whereas those from the as-synthesized ZSM-52 (as well as as-synthesized ZSM-55) are very sharp and extend to higher resolution. Using a shape transform argument,[23] the broadening of the diffraction peaks from the calcined form, obscuring, for example, a peak doublet near $d = 7$ Å, indicates that the crystallite sizes of ordered regions are quite small. A similar broadening effect is observed for calcined MCM-47, for which reflections extend to a similar resolution. (Indeed, the powder pattern from calcined ZSM-52 greatly resembles that obtained from MCM-47 subjected to the "procedure A" calcination described by Burton et al.[9] and depicted in their Figure 2b.)

A similar dependence of ease of calcination on SDA used for synthesis was mentioned in a study of ZSM-18.[20] The close fit of the template to the channel opening in this example indicates an intimate geometric effect as the organic material directs the synthesis of the aluminosilicate cage. Subsequent removal also seems to be a function of template type.[24,25] How such interactions might be important to the MCM-65/MCM-47/ZSM-52/ZSM-55 calcinations can only be speculated at this stage. Quinuclidine is a compact molecule that can display spherical disorder in the solid state.[26] However MCM-65 is also made with a tetramethylammonium hydroxide co-component. The dipyrolidinium diquat template used to prepare MCM-47,

on the other hand, would be more dumbbell-shaped, as modeled for this crystal structure,[9] whereas the conformational geometry of choline chloride in either ZSM-52 or ZSM-55 is unknown. The expanded *a*-axis dimension, however, indicates a somewhat different precursor structure.

It is clear that MCM-65, MCM-47, ZSM-52, and ZSM-55 represent a family of very similar layered materials with an underlying ferrierite layer substructure that however, is different from ferrierite itself. Given a suitable SDA, therefore, a crystalline material is formed that links all silanol groups. Otherwise, a disordered material is produced upon calcination. It seems unlikely that extensive lateral shifts of ferrierite sublayers along the *b* axis are involved in the disorder process as this would change the overall diffraction symmetry, something that is not observed experimentally.

Acknowledgment. Drs. Sandeep S. Dhingra, Guang Cao, and James Vartuli are thanked for providing samples and powder diffraction data used in this study. The skillful assistance of Mr. Clarence E. Chase in recording the NMR data is gratefully acknowledged. Mr. Karl Strohmaier, Dr. Wieslaw Roth, and Dr. James Vartuli are thanked for helpful discussions.

References and Notes

(1) Szostak, R. S. *Molecular Sieves*, 2nd ed.; Blackie Academic & Professional: London, 1998.

(2) Leonowicz, M. E.; Lawton, J. A.; Lawton, S. L.; Rubin, M. K. *Science* **1994**, *264*, 1910.

(3) Camblor, M. A.; Corma, A.; Diaz-Cabanas, M. J.; Baerlocher, C. *J. Phys. Chem. B* **1998**, *102*, 44.

(4) Lawton, S. L.; Fung, A. S.; Kennedy, G. J.; Alemanny, L. B.; Chung, C. D.; Hatzikos, G. H.; Lissy, D. N.; Rubin, M. K.; Timken, H. K. C.; Steuernagel, S.; Woessner, D. E. *J. Phys. Chem.* 1996, *100*, 3788.

(5) Dorset, D. L. *Z. Kristallogr*. **2003**, *218*, 612.

(6) Vaughan, P. A. *Acta Crystallogr*. **1966**, *21*, 983.

(7) Schreyeck, L.; Caullet, P.; Mongenel, J. C.; Guth, J. L.; Marler, B. *Microporous Mater*. **1996**, *6*, 259.

(8) Valyocsik, E. W. U.S. Patent 5,068,096, 1991.

(9) Burton, A.; Accardi, R. J.; Lobo, R. F.; Falconi, M.; Deem, M. W. *Chem. Mater*. **2000**, *12*, 2936.

(10) Kresge, C. T.; Casmer, S. G.; Dhingra, S. World Patent WO 02/42208 A1, 2002.

(11) Chu, P.; Herbst, J. A.; Klocke, D. J.; Vartuli, J. U.S. Patent 4,-985,223, 1991.

(12) Rubin, M. K. U.S. Patent 5,063,037, 1991.

(13) Larsson, A. C.; von Dreele, R. B. *General Structure Analysis System, GSAS*; Los Alamos Laboratory: Los Alamos, NM, 1994.

(14) Baerlocher, C.; Hepp, A.; Meier, W. M. *Distance Least Squares Refinement Program, DLS-76*; ETH: Zurich, Swizerland, 1977.

(15) Zou, X. D.; Sukharev, Yu.; Hovmöller, S. *Ultramicroscopy* **1993**, *49*, 147.

(16) Hauptman, H. A. *Crystal Structure Determination. The Role of the Cosine Seminvariants*; Plenum Press: New York, 1972.

(17) Cowley, J. M.; Rees, A. L. G.; Spink, J. A. *Proc. Phys. Soc. (London)* **1951**, *A64*, 609.

(18) Dorset, D. L. *Z. Kristallogr*. **2003**, *218*, 237.

(19) Baerlocher, C.; Meier, W. M.; Olson, D. H. *Atlas of Zeolite Framework Types*; Elsevier: Amsterdam, 2001.

(20) Lawton, S. L.; Rohrbaugh, W. J. *Science* **1990**, *247*, 1319.

(21) Lawton, S. L. Unpublished data.

(22) Bondi, A. *J. Phys. Chem*. **1964**, *68*, 441.

(23) Dorset, D. L. *Structural Electron Crystallography*; Plenum Press: New York, 1995.

(24) Schmitt, K. D.; Kennedy, G. J. *Zeolites* **1994**, *14*, 635.

(25) Schmitt, K. D. U.S. Patent 5,350,570, 1994

(26) Nowacki, W. *Helv. Chim. Acta* **1946**, *29*, 1798.

(27) Meier, W. M.; Moeck, H. J. *J. Solid State Chem*. **1979**, *27*, 349.

(28) O'Keeffe, M.; Hyde, S. T. *Zeolites* **1997**, *19*, 370.